Symmetric Behavior of Hemoglobin α- and β- Subunits during Acid-Induced Denaturation Observed by Electrospray Mass Spectrometry†

Brian L. Boys, Mark C. Kuprowski, and Lars Konermann*

Department of Chemistry, The University of Western Ontario, London, Ontario N6A 5B7, Canada

Received June 2, 2007; Revised Manuscript Received July 10, 2007

ABSTRACT: This work employs electrospray mass spectrometry (ESI-MS) and UV−vis spectroscopy for monitoring the mechanism of acid-induced hemoglobin (Hb) denaturation. The protein for these experiments has been freshly prepared from bovine blood. All three Hb derivatives studied (^{oxy}Hb, ^{met}Hb, and ^{cyanomet}Hb) respond to gradual changes from pH 6.8 to 2.1 in a manner that can be described by a stepwise sequential unfolding mechanism: $(\alpha^h\beta^h)_2 \rightarrow 2\ \alpha^h\beta^h \rightarrow 2\ \alpha^h_{folded} + 2\ \beta^h_{folded} \rightarrow 2\ \alpha^a_{unfolded} + 2\ \beta^a_{unfolded} + 4$ heme (superscripts "h" and "a" refer to holo- and apo-forms, respectively). The results obtained on these freshly prepared samples are significantly different from those of similar experiments previously conducted on ^{met}Hb obtained commercially as lyophilized powder. Those earlier experiments suggested a highly asymmetric behavior of the two globin chains, involving a heme-deficient dimer ($\alpha^h\beta^a$) as a mechanistically important intermediate on the (dis)assembly pathway. Importantly, heme-deficient dimers are virtually undetectable for the freshly prepared Hb derivatives studied herein at any pH. This apparent discrepancy is attributed to the occurrence of oxidative modifications in the commercial protein. Liquid chromatography and tandem mass spectrometry reveal significant levels of sulfoxide formation for all four methionine residues in commercially obtained ^{met}Hb. The extent of these modifications for freshly prepared protein is lower by at least a factor of 10. It is concluded that the acid-induced denaturation of Hb follows a highly symmetric mechanism. The occurrence of other mechanisms (possibly involving asymmetric elements) under different solvent conditions cannot be ruled out.

Hemoglobin A (Hb[1]) is a highly conserved oxygen transport protein found in mammalian red blood cells (RBCs) at a tetramer concentration around 5 mM (*1*). Hb is composed of two heme-containing α- and β-globin dimers (αβ) arranged in a tetrahedral dimer of dimers fashion (*2*, *3*). Vertebrate α- and β-globins share roughly 50% sequence homology (*4*). The α- and β-subunits are equally divergent from the oxygen storage protein myoglobin, with a globin fold comprising seven and eight helices, respectively (*4*, *5*). The noncovalent contacts that stabilize tetrameric Hb are located along two distinct interfaces and encompass nonpolar and van der Waals interactions, hydrogen bonds, and salt bridges (*5*). α- and β-subunits interacting along the $\alpha_1\beta_1$ ($\alpha_2\beta_2$) packing interface form contacts that involve some 34 residues (*6*−*8*). The $\alpha_1\beta_2$ ($\alpha_2\beta_1$) sliding interface is characterized by somewhat weaker contacts, involving only about 19 residues (*2*, *8*). The specific architecture of this $\alpha_1\beta_2$ ($\alpha_2\beta_1$) interface provides the structural basis for cooperative oxygen binding. More extensive salt bridges are present in the T (tense) or deoxy state than in the R (relaxed) or oxy state (*3*). This structural change leads to a remarkable increase in the tetramer−dimer dissociation constant upon oxygenation, from ca. 10^{-11} M in the T state to ca. 10^{-6} M in the R state (*1*, *9*).

Hb also serves as an important model system for exploring the mechanisms by which multi-subunit complexes assemble from their monomeric constituents. Studies of this kind have been carried out *in vitro* (*10*−*12*) and in cell-free systems (*13*) as well as *in vivo* (*14*). A total of eight moieties, namely, two apo-α-chains (α^a), two apo-β-chains (β^a), and four heme groups are required for the formation of the intact $(\alpha^h\beta^h)_2$ tetramer (superscripts a and h refer to apo- and heme-bound holo states, respectively). For many previous *in vitro* experiments, the assembly of Hb has been triggered by mixing initially separated α^h and β^h subunits under native solvent conditions. Prior to mixing, the isolated subunits form noncovalent $(\alpha^h)_2$ and $(\beta^h)_4$ complexes, respectively. The dissociation of these species into monomers allows the formation of αβ heterodimers to occur, which can then form the native $(\alpha^h\beta^h)_2$ structure (*10*, *15*−*19*). Electrostatic interactions play an important role in guiding these assembly processes (*20*−*22*). The *in vivo* mechanism of Hb formation likely involves co-translational folding and heme binding of the individual subunits. A chaperone (AHSP, α-hemoglobin-stabilizing protein) binds to nascent monomeric α^h, thereby preventing the formation of cytotoxic α-globin aggregates (*8*, *23*−*28*). Interestingly, the assembly of intact ^{met}Hb from extensively unfolded monomeric subunits and free heme can

† This work was supported by the Natural Sciences and Engineering Research Council of Canada (NSERC), the Canada Foundation for Innovation (CFI), and the Canada Research Chairs Program.

* To whom correspondence should be addressed. Tel: (519) 661-2111 ext. 86313. Fax: (519) 661-3022. E-mail: konerman@uwo.ca.

[1] Abbreviations: α^a, apo-α-globin; β^a, apo-β-globin; β^a_{ox}, oxidatively damaged apo-β-globin; α^h, holo-α-globin; β^h, holo-β-globin; DPG, 2-3-diphosphoglycerate; ESI-MS, electrospray ionization mass spectrometry; Hb, hemoglobin; ^{cyanomet}Hb, ferri (Fe^{3+}) hemoglobin with heme iron ligated by CN^- in the distal position; ^{met}Hb, ferri (Fe^{3+}) hemoglobin; ^{oxy}Hb, ferro (Fe^{2+}) hemoglobin with heme iron ligated by O_2 in the distal position; LC, liquid chromatography; RBC, red blood cell.

10.1021/bi701076q CCC: $37.00
Published on Web 08/24/2007

proceed *in vitro* even in the absence of AHSP (*29*). The overall picture that emerges from these previous studies as well as from equilibrium experiments (*7*) is that the Hb assembly mechanism follows the general sequence $2\ \alpha + 2\ \beta \rightarrow 2\ \alpha\beta \rightarrow (\alpha\beta)_2$ (*23*, *30*, *31*). It is undisputed that native $(\alpha^h\beta^h)_2$ is generated by the binding of two $\alpha^h\beta^h$ heterodimers to each other. However, the question whether $\alpha^h\beta^h$ is preceded by another heterodimeric species is still a matter of debate (*32*). Soret absorption measurements and other spectroscopic experiments suggest that the assembly process at near-neutral pH may involve semi-α-hemoglobin ($\alpha^h\beta^a$) as a major intermediate for both human and bovine Hb (*13*, *32*−*37*).

In principle, both α- and *β*-globin can exist in various conformations, heme binding states, and quaternary structures, thus resulting in a vast number of possible species that could potentially be involved in the assembly process. On the basis of conventional spectroscopic measurements, it is challenging to obtain clear-cut evidence for the existence of specific reaction pathways and to prove or disprove the existence of certain intermediates. Electrospray ionization (ESI) mass spectrometry (MS), however, is a highly selective technique that allows the detection of multiple coexisting protein species (*38*). The gentle nature of the ESI process implies that intact ligand−protein and protein−protein complexes can be transferred into the gas phase such that the composition of these assemblies can be deduced from their mass (*38*−*43*). At the same time, the charge-state distributions of the observed protein ions provide information on the overall compactness of the corresponding solution-phase conformations. Unfolded proteins generally result in higher protonation states than tightly folded conformers (*38*, *44*, *45*).

In an interesting study, Griffith and Kaltashov (*46*) recently employed ESI-MS for monitoring the response of ^{met}Hb to increasing acid concentrations. A stepwise decrease in pH from 8 to 3 resulted in a gradual decay of the $(\alpha^h\beta^h)_2$ signal. α^h and $\alpha^h\beta^h$ were the major species observed around pH 5. Below pH 4, unfolded α^a and β^a chains were dominant. These experiments suggested characteristic differences in the behavior of α- and *β*-globin. The former was able to bind heme independent of its association state, apparent by the observation of monomeric α^h. In contrast, monomeric *β*-globin was seen exclusively in its apo-state. On the basis of these observations, it was proposed that *β*-globin exhibits heme-binding competency only while in association with α^h chains, in either a dimeric or tetrameric complex. Another notable result was the observation of a heme-deficient dimer ($\alpha^h\beta^a$), which was interpreted as a key intermediate of the (dis)assembly process. It was suggested that the apparent asymmetric behavior of the two subunits during acid-induced unfolding might have general implications for the assembly of Hb under nondenaturing conditions both *in vitro* and *in vivo* (*35*, *46*, *47*). A subsequent study from our laboratory came to somewhat different conclusions. Upon monitoring the refolding of ^{met}Hb at slightly basic pH, it was found that both monomeric α- and *β*-globin were capable of binding heme. Moreover, these refolding data did not support the notion that $\alpha^h\beta^a$ is an obligatory intermediate en route toward the native $(\alpha^h\beta^h)_2$ complex (*29*).

Most biochemical experiments on Hb that have been performed since the 1950s employed protein that had been freshly prepared from RBCs. This is in contrast to quite a number of more recent ESI-MS studies that were based on Hb obtained commercially as lyophilized powder (*29*, *47*−*52*). In particular, experiments on commercial protein provided the basis for the proposed asymmetric unfolding mechanism of Hb at acidic pH (*35*, *46*). It has been noted earlier that commercial Hb contains significant levels of chemical modifications (*52*, *53*). While studies on these samples can undoubtedly provide interesting information, it is imperative to explore how far the history of the protein affects its biochemical properties. This work revisits the mechanism of acid-induced Hb denaturation. Using ESI-MS, we show that the behavior of freshly prepared Hb is dramatically different from that of protein from commercial sources. We study the response to changes in pH for three forms, ^{oxy}Hb (oxygen-bound with heme iron in the Fe^{2+} oxidation state), ^{met}Hb (physiologically inactive, with heme iron in the Fe^{3+} oxidation state), and ^{cyanomet}Hb (^{met}Hb with heme iron distally ligated by CN^-) (*5*). The pH profiles obtained in this way reveal a remarkably symmetrical behavior for both α- and *β*-globin, with $\alpha^h\beta^a$ dimers being virtually undetectable under any conditions.

EXPERIMENTAL PROCEDURES

Materials. Bovine ^{oxy}Hb was prepared from fresh hemolysate via standard procedures (*5*). Briefly, fresh blood was collected from a Holstein heifer (*54*) using sterile intravenous techniques into a chilled glass vial containing sodium citrate as an anticoagulant to a final concentration of 0.3% (w/v). Centrifugation at 5,500*g* for 20 min gave a RBC pellet. Plasma and buffy coat (containing white blood cells and platelets) were removed with suction. Isolated RBCs were resuspended and washed in isotonic 0.9% (w/v) sodium chloride and then centrifuged again at 5,500*g* for 20 min. This washing step was repeated four times to rid the samples of plasma proteins and cellular debris. Hemolysate was obtained through osmotic shock, and stromal impurities were extracted into an organic phase. This was achieved by mixing the packed RBCs with an equal volume of distilled water containing 10% (v/v) toluene. Centrifugation at 15,000*g* for 30 min yielded an aqueous layer of purified hemolysate, which was then dialyzed at 4 °C against 10 mM ammonium acetate over a period of 36 h with multiple buffer exchanges. The total concentration of the purified ^{oxy}Hb stock solution obtained in this way was determined via the pyridine hemochromogen method to be 1.7 mM (as tetramer) (*55*). Analyses employing UV−vis spectroscopy on ^{cyanomet}Hb with, $\epsilon_{540} = 44\ mM^{-1}\ cm^{-1}$ (as tetramer), were in agreement with this result (*56*, *57*). In contrast to human Hb, the bovine protein interacts only weakly with 2−3-diphosphoglycerate (DPG), and the 2−3-DPG levels in bovine RBCs are relatively low (*58*, *59*). Inductively coupled plasma MS revealed that the dialysis procedure outlined above further lowered the concentration of organophosphates in the hemolysate by roughly 1 order of magnitude. In order to minimize auto-oxidation of ^{oxy}Hb to ^{met}Hb, the protein stock solutions were flash frozen in liquid nitrogen in 10 mM ammonium acetate. Rapid thawing was practiced in accordance with previous studies (*60*). The percentage of ^{met}Hb in the thawed ^{oxy}Hb stock solutions was ca. 2%, as determined by measuring the absorbance decrease at 620 nm upon addition of KCN (*61*−*63*). Aliquots of freshly prepared

^{oxy}Hb were purposely converted to ^{met}Hb by oxidation with a 1.2-fold stoichiometric excess of potassium ferricyanide for 5 min at 25 °C. A fraction of the ^{met}Hb was then further derivatized to ^{cyanomet}Hb by exposing it to a 1.2-fold stoichiometric excess of neutralized potassium cyanide for 2 min at 25 °C. All derivatized Hb species were desalted on a 3 × 25 cm G-25 Sephadex column prior to analysis.

Commercial bovine ^{met}Hb was purchased from Sigma (St. Louis, MO). The purification procedure used by this manufacturer (*64*) is similar to that outlined above, except that the protein was lyophilized after purification. Stock solutions were generated from the lyophilized powder by dissolving it in 10 mM ammonium acetate at a concentration 1 mM (as tetramer). Subsequently, these solutions were dialyzed against 10 mM ammonium acetate. Small amounts of insoluble debris were removed by centrifugation. Post-dialysis samples were flash frozen in liquid nitrogen and stored at −80 °C. The percentage of ^{met}Hb in the commercially obtained stock was found to be around 99%. All experiments in this work were carried out on Hb solutions containing ammonium acetate at a final concentration of 10 mM. Absorption measurements were performed on a Carry-300 Varian UV−vis spectrophotometer (Palo Alto, CA), using a protein concentration of 15 μM (as tetramer) and a cuvette with a 1 mm optical path length.

Mass Spectrometry. Mass spectra were recorded on a Q-TOF Ultima API instrument (Waters/Micromass, Manchester, UK) utilizing a standard Z-spray ESI source operating in positive ion mode. All MS parameters were optimized to give the highest Hb tetramer signal at pH 6.8. A capillary voltage of 3.5 kV, a cone voltage of 45 V, and an RF lens 1 voltage of 20 V were found to be optimal. The desolvation and source temperatures were kept low (30 and 80 °C, respectively) to minimize tetramer dissociation. Samples were introduced into the mass spectrometer at a flow rate of 5 μL min^{-1} via a syringe pump. Hb samples analyzed by ESI-MS were of high concentration (60 μM as tetramer) to minimize the dissociation of noncovalent complexes in solution. All Hb samples were diluted from the corresponding stock solution, and the pH was adjusted with formic acid, allowing an equilibration period of 1 h prior to analysis. The mass spectrometer was calibrated with CsI. The ion optics were adjusted to provide uniform transmission in the *m*/*z* range of interest. All data were acquired and analyzed using MassLynx software provided by the instrument manufacturer. Consistent with previous reports, the subunit masses of the protein were found to be 15,053 and 15,954 Da for α^a and β^a, respectively (*50*, *65*). The heme prosthetic group accounts for an additional 616 Da for each subunit.

The locations of oxidative modification sites in commercial ^{met}Hb were determined by tryptic peptide mapping and LC-ESI-MS/MS. Fifty micromolar ^{met}Hb was digested with trypsin for 4 h at 37 °C using a 10:1 ^{met}Hb/trypsin ratio by weight. The digest was loaded into a 25 μL sample loop and separated on a Symmetry 300 C18 column (2.1 100 mm, Waters). The 1525 μm pump (Waters) employed for these HPLC experiments was operated at a flow rate of 100 μL min^{-1}, with a linear water/acetonitrile gradient in the presence of 0.05% trifluoroacetic acid. The acetonitrile content of the mobile phase was ramped from 2% to 60% within 60 min. Peptides of interest were analyzed by ESI-MS/MS as they eluted from the column by operating the Q-TOF in data-dependent acquisition mode.

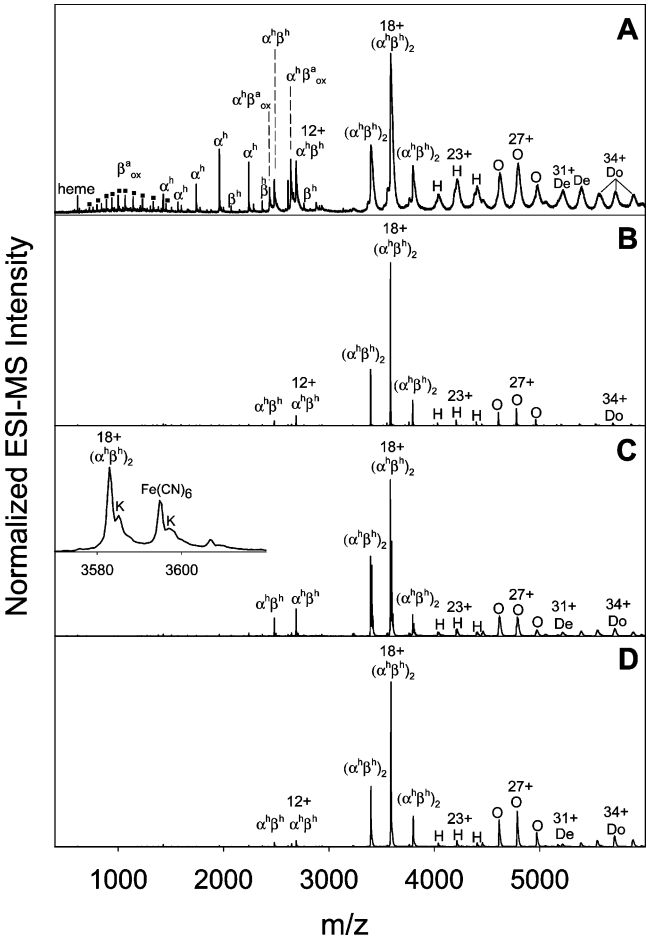

FIGURE 1: ESI mass spectra of different Hb derivatives recorded under native solvent conditions (pH 6.8) at a tetramer concentration of 60 μM. (A) ^{met}Hb obtained commercially as a lyophilized powder. The other three panels show data for Hb freshly prepared from bovine blood: (B) ^{oxy}Hb; (C) ^{met}Hb; and (D) ^{cyanomet}Hb. Notation: H, O, De, Do are hexamers, octamers, decamers, and dodecamers, respectively. Peaks labeled with black squares represent the (apo-β +32) Da species ($\beta^a{}_{ox}$). The inset in (C) shows a ferrocyanide and potassium (K) adduct bound to ^{met}Hb tetramers.

RESULTS AND DISCUSSION

Comparison of Different Hemoglobin Samples. The ESI mass spectrum recorded for commercially obtained ^{met}Hb at pH 6.8 (Figure 1A) resembles data reported in previous ESI-MS studies (*46*, *52*). It shows a host of different species, including $(\alpha^h\beta^h)_2$ tetramers, $\alpha^h\beta^h$ dimers, heme-deficient dimers ($\alpha^h\beta^a{}_{ox}$), and monomeric α^h, β^h, and $\beta^a{}_{ox}$ as well as free heme. The subscript ox is used for ions exhibiting a molecular mass that is 32 Da higher than expected on the basis of their amino acid sequence. This phenomenon is attributed to oxidative modifications (*29*, *52*), as discussed in more detail below. The occurrence of a tetramer−dimer equilibrium for ^{met}Hb is well established (*7*, *66*, *67*) such that the observation of dimeric species in Figure 1A is not surprising. A K_d value of 4 μM has been reported for the MetHb $(\alpha^h\beta^h)_2 \leftrightarrow 2\ \alpha^h\beta^h$ dissociation, whereas the corresponding value for ^{cyanomet}Hb is 1 μM at pH 7 (*9*). However, the presence of significant amounts of monomeric globin ions in Figure 1A is unexpected, considering the results of

previous experiments carried out in bulk solution (*7*, *66*, *67*). It might be suspected that some of the monomeric and dimeric species in the spectrum are fragmentation products generated during ESI, but recent hydrogen/deuterium exchange studies have shown this not to be the case. Instead, all of the ionic signals mentioned so far correspond to protein species that exist in solution (*53*). Figure 1A also reveals the presence of hexamers $(\alpha^h\beta^h)_3$, octamers $(\alpha^h\beta^h)_4$, decamers $(\alpha^h\beta^h)_5$, and dodecamers $(\alpha^h\beta^h)_6$. Although there is evidence for the possible formation of higher order Hb assemblies under some conditions (*1*), $(\alpha^h\beta^h)_n$ species with $n > 2$ observed here likely represent clusters generated during ionization, a common occurrence in ESI-MS (*53*, *68*, *69*). Somewhat surprisingly, the relative contributions of these large assemblies were not strongly dependent on the protein concentration used. Decreasing the concentration by a factor of 10, or increasing it 2-fold, resulted in hexamer to dodecamer intensities similar to those in Figure 1A (data not shown).

Compared to the data for commercial ^{met}Hb, the ESI mass spectrum of freshly prepared ^{oxy}Hb has a much simpler appearance (Figure 1B), being strongly dominated by $(\alpha^h\beta^h)_2$ ions. The contributions of $\alpha^h\beta^h$ and larger aggregates are greatly reduced. Monomeric species as well as heme-deficient dimers are virtually undetectable. The measured mass corresponds to that of de-oxygenated Hb, that is, O_2 binding is not maintained during the ESI process, although the protein is infused into the ion source in its fully oxygenated form. The peak width is significantly reduced because of vast improvements in desolvation behavior. Signal broadening caused by the presence of residual solvent adducts is frequently observed in ESI mass spectra of large noncovalent complexes, as exemplified in Figure 1A (*40*, *70*, *71*). The observation of much more favorable desolvation properties for freshly prepared ^{oxy}Hb (Figure 1B) is remarkable. To investigate whether the different ESI-MS behavior of the two samples is related to the oxidation state of the heme iron, freshly prepared ^{oxy}Hb was converted to ^{met}Hb by exposure of the protein to potassium ferricyanide. The resulting spectrum (Figure 1C) is very similar to that obtained for ^{oxy}Hb, albeit with slightly elevated intensities for dimers and larger aggregates (hexamer to dodecamer). Close inspection of the tetramer signals reveals peak splitting due to a residual $Fe(CN)_6$ adduct (Figure 1C, inset). This behavior is consistent with the known tendency of Hb to accommodate ferrocyanide in its organophosphate binding site, which lies between the two β-subunits in the tetrameric complex (*5*, *72*). Dimers do not possess this binding site, consistent with the observation that $\alpha^h\beta^h$ does not form a ferrocyanide adduct. For completeness, we also investigated the properties of ^{cyanomet}Hb, which was obtained by incubation of ^{met}Hb with a slight molar excess of neutralized KCN (see the Experimental Procedures section). The overall differences between the ESI mass spectra of freshly prepared ^{cyanomet}Hb (Figure 1D) and ^{met}Hb (Figure 1C) are relatively small. However, Figure 1D shows a lower contribution of $\alpha^h\beta^h$, consistent with the fact that heme ligation with CN^- reduces the K_d of $(\alpha^h\beta^h)_2$ by a factor of 4, as mentioned above (*9*).

In additional experiments, freshly prepared ^{oxy}Hb was lyophilized, followed by redissolution and extended storage of the resulting samples. Mass spectra obtained for protein treated in this way resembled that of commercial ^{met}Hb (Figure 1A), with prominent monomer, dimer, and $\alpha^h\beta^a{}_{ox}$ signals (data not shown).

Acid-Induced Denaturation. Figure 2 depicts the changes in the ESI mass spectrum upon acidification of freshly prepared ^{oxy}Hb. Lowering the pH from 6.8 to 4.4 (Figure 2A and B) results in a dramatic shift of the tetramer−dimer equilibrium such that $\alpha^h\beta^h$ becomes the dominant species. In addition, ionic signals corresponding to monomeric α^h and β^h are observed. The low charge states (around 7+) of these monomer ions indicate that they represent highly compact protein conformers in solution (*45*, *73*). Upon decreasing the pH to 4.0, the relative signal intensities of α^h and β^h increase further. At the same time, highly charged α^a and β^a ions appear in the spectrum, indicating the presence of significantly unfolded apo-globin chains in solution (Figure 2C). This trend continues upon further acidification (Figure 2D). Figure 2E represents the end point of the titration. The spectrum under these conditions (pH 2.1) exclusively shows α^a and β^a ions, with charge-state distributions that have their maxima around 17+. These data reflect the fact that at pH 2.1 all quaternary contacts and heme−protein interactions have been disrupted and that the monomeric subunits are extensively unfolded in solution (*45*, *73*). The higher signal intensities for α^a than for β^a can be attributed to ion suppression effects as well as to differences in the desolvation behavior of the two globin chains (*74*). The heme released during denaturation is not detectable in Figure 2C−E because of the rapid aggregation of the free porphyrin under acidic conditions (*75*, *76*). ESI mass spectra very similar to those depicted in Figure 2 were obtained during the acid-induced denaturation of freshly prepared ^{met}Hb and ^{cyanomet}Hb, demonstrating that the overall denaturation mechanism of the three forms studied here is largely insensitive to changes in heme oxidation and ligation state. Detailed ESI-MS titration data for the two ferri Hb derivatives are not shown because of space limitations; however, selected spectra for ^{met}Hb will be discussed below (Figure 7).

Complementary information on the acid-induced denaturation of the three freshly prepared Hb derivatives can be obtained by UV−vis spectroscopy. The absorbance changes accompanying the titration of ^{oxy}Hb are depicted in Figure 3. At neutral pH, the protein shows bands at 577 and 541 nm and a dominant Soret signal at 415 nm. The presence of these so-called α, β, and γ bands confirms that the protein is indeed in its fully oxygenated low-spin Fe^{2+} state (*5*). Acidification leads to a gradual disappearance of the 577/541 nm doublet, and the Soret peak shifts to 405 nm. This spectral transition reflects a change in formal heme oxidation state to Fe^{3+}, corresponding to that of ^{met}Hb. The onset of this process occurs around pH 4, that is, in the range where monomeric α^h, β^h, and free apoprotein start to occur in the ESI mass spectrum (Figure 2C). These changes reflect the fact that the highly specific structural environment of the native heme binding pocket in ^{oxy}Hb protects the heme iron from autoxidation (*77*). Disruption of the binding pocket during denaturation allows the $Fe^{2+} \rightarrow Fe^{3+}$ transition to occur under the aerobic solution conditions used here. Further acidification leads to a broad spectrum that is blue shifted even further, characteristic of heme that has been released from the protein and has undergone acid aggregation (*78*−*80*).

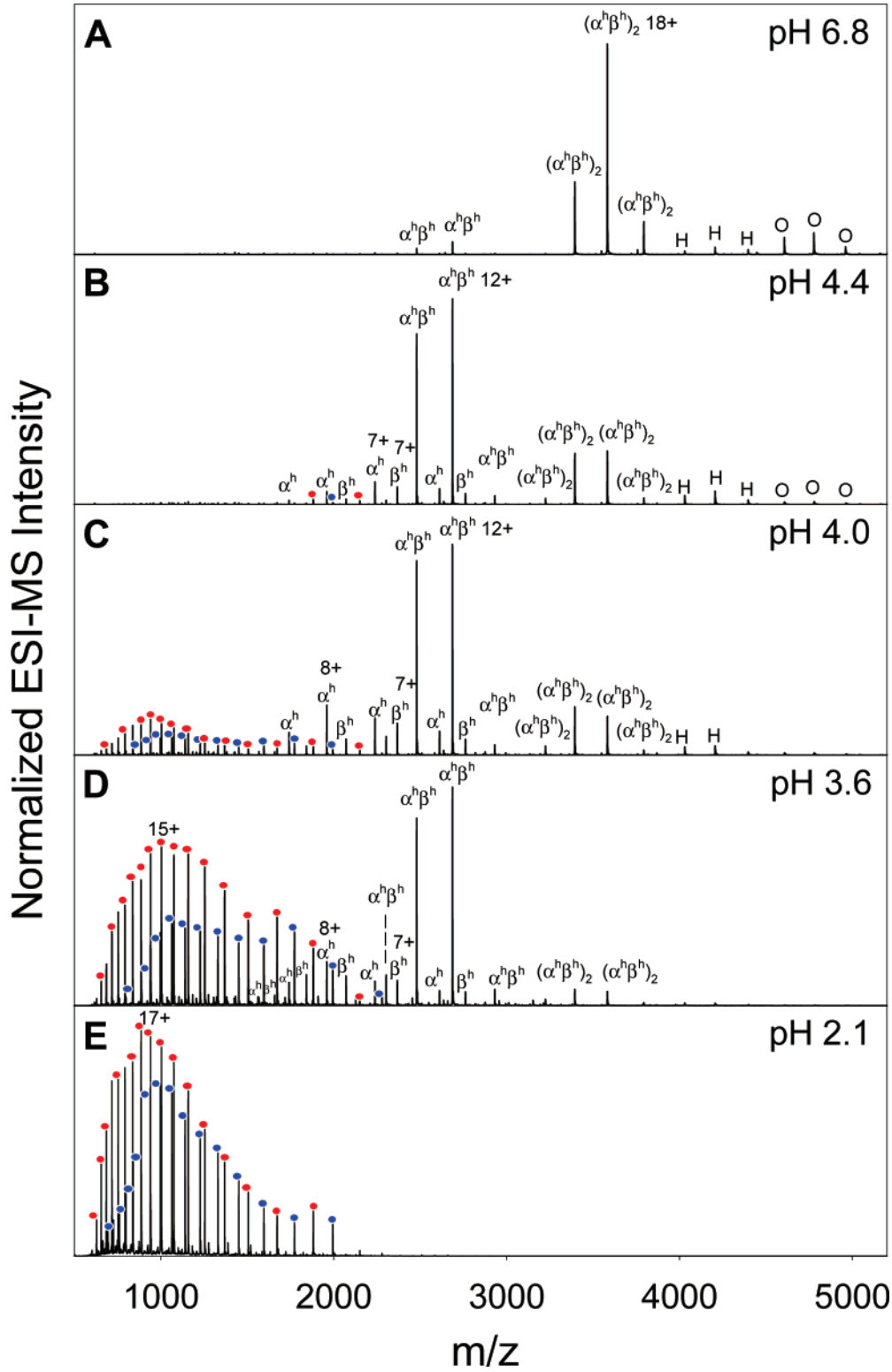

FIGURE 2: ESI mass spectra of freshly prepared ^{oxy}Hb recorded at different pH (as indicated). Notation: the same as that in Figure 1; the red and blue symbols represent α^a and β^a ions, respectively. The charge states of selected ions are indicated.

The spectral changes accompanying the acid-induced denaturation of freshly prepared ^{met}Hb exhibit an isosbestic point at 380 nm (Figure 4). This suggests that the ferri-heme chromophore experiences a two-state transition, from protein-bound to aggregated in acidic solution. Since these spectral changes only probe the heme environment, the apparent two-state nature of the optical transition does not contradict the observation of various protein oligomerization states (monomers, dimers, and tetramers) by ESI-MS. In the range between pH 4 and pH 2.1, the data for ^{cyanomet}Hb (Figure 5) are very similar to those for ^{met}Hb (Figure 4), reflecting the transition from protein-bound ferri-heme to the acid-denatured state of Hb. In the case of ^{cyanomet}Hb, however, this process is preceded by the loss of cyanide, apparent from an absorbance decrease around 540 nm, as well as a shift of the Soret band from 419 to 405 nm (Figure 5) (*5*). Presumably, the driving force for this reaction is the protonation of cyanide at low pH. This cyanide loss is a

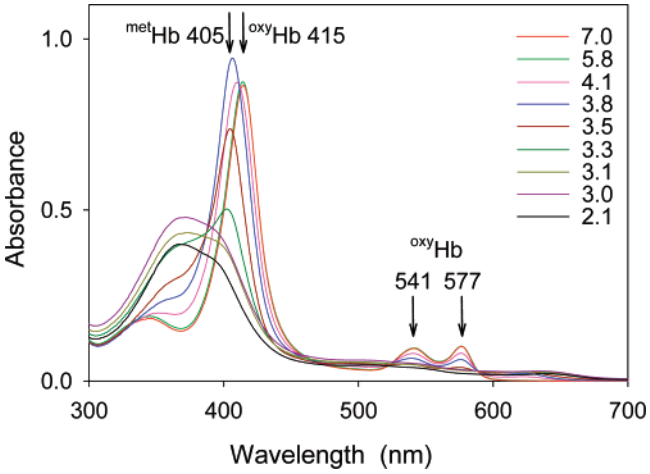

FIGURE 3: UV−vis spectral changes accompanying the acid-induced denaturation of freshly prepared ^{oxy}Hb. The pH values for the individual spectra are indicated. Also shown are the characteristic absorption maxima for ^{oxy}Hb and ^{met}Hb (*5*).

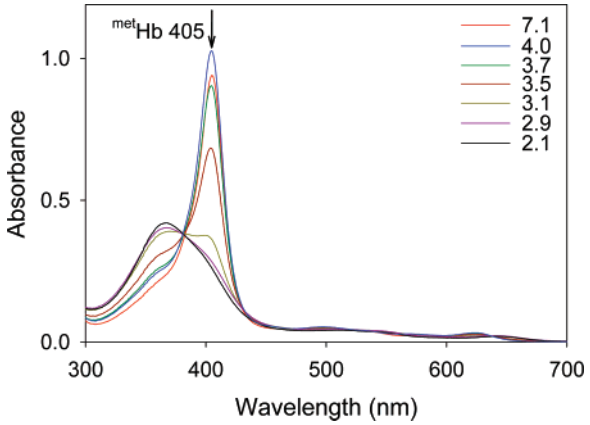

FIGURE 4: UV−vis spectral changes accompanying the acid-induced denaturation of freshly prepared ^{met}Hb.

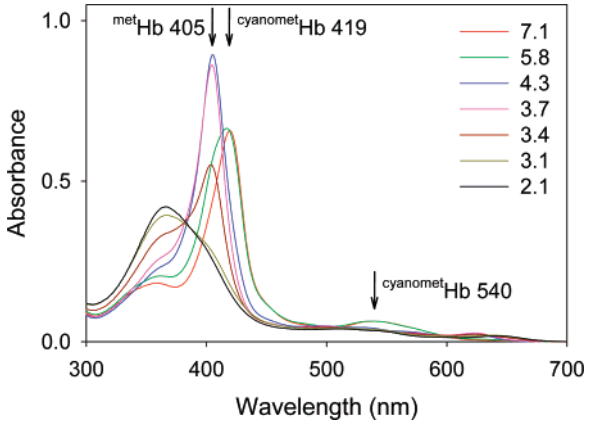

FIGURE 5: UV−vis spectral changes accompanying the acid-induced denaturation of freshly prepared ^{cyanomet}Hb. Also shown are the characteristic absorption maxima for ^{met}Hb and ^{cyanomet}Hb (*5*).

gradual process that can be monitored directly by ESI-MS (Figure 6). In the near-neutral range, the mass spectra show $(\alpha^h\beta^h)_2$ bound to up to four CN^- groups. Acidification induces a gradual shift of the distribution, until at pH 3.5 the base peak corresponds to the mass of unligated $(\alpha^h\beta^h)_2$. Because protonation is an integral part of the ionization process, it is possible that some cyanide is released in the form of HCN during ESI. Thus, the distributions in Figure

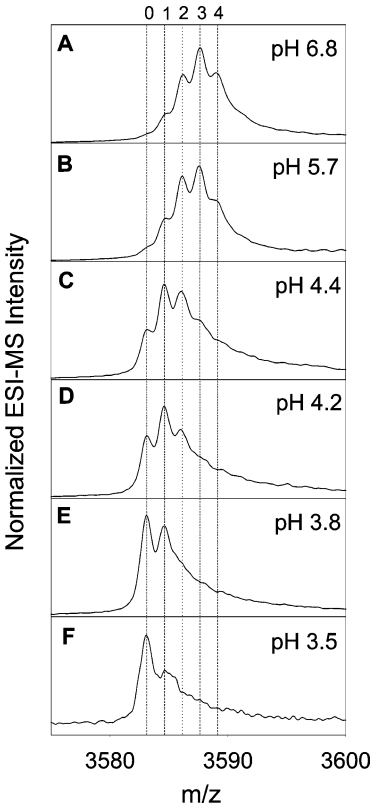

FIGURE 6: Partial ESI mass spectra showing the $(\alpha^h\beta^h)_2$ 18+ region of freshly prepared ^{cyanomet}Hb at different pH values. The dotted lines numbered 0 through 4 indicate the number of cyano groups bound to the protein tetramer. The changes in the overall spectrum as a function of pH are very similar to those depicted in Figure 2.

6 likely under-represent the actual cyanide binding levels in bulk solution. No cyanide binding was observed for dimeric or monomeric globins.

A key conclusion from the acid-induced denaturation data presented so far (especially those in Figures 1 and 2) is that the α- and β-subunits of freshly prepared Hb exhibit a highly symmetric behavior: changes in association state, heme binding, and conformation exhibited by α-globin are closely mirrored by the β-subunit. On the basis of Figure 2, the denaturation process can be summarized by the following simplified scheme (ignoring the possible involvement of higher order aggregates):

$$(\alpha^h\beta^h)_2 \rightarrow 2\,\alpha^h\beta^h \rightarrow$$
$$2\,\alpha^h{}_{folded} + 2\,\beta^h{}_{folded} \rightarrow \qquad \text{(Scheme1)}$$
$$2\,\alpha^a{}_{unfolded} + 2\,\beta^a{}_{unfolded} + 4\ \text{heme}$$

This result contrasts the data previously obtained on commercial ^{met}Hb, which indicate highly asymmetric behavior of the two subunits, as discussed in the Introduction section (*46*).

A particularly striking result in previous studies on commercial ^{met}Hb was the observation of an $\alpha^h\beta^a$ dimer during acid-induced denaturation (*46*). It was proposed that this species represents a mechanistically important intermediate during the (dis)assembly process of the native tetramer (*35*, *46*, *47*). The spectrum depicted in Figure 1A confirms the existence of a heme-deficient heterodimer for the commercial protein at pH 6.8, albeit with a +32 Da

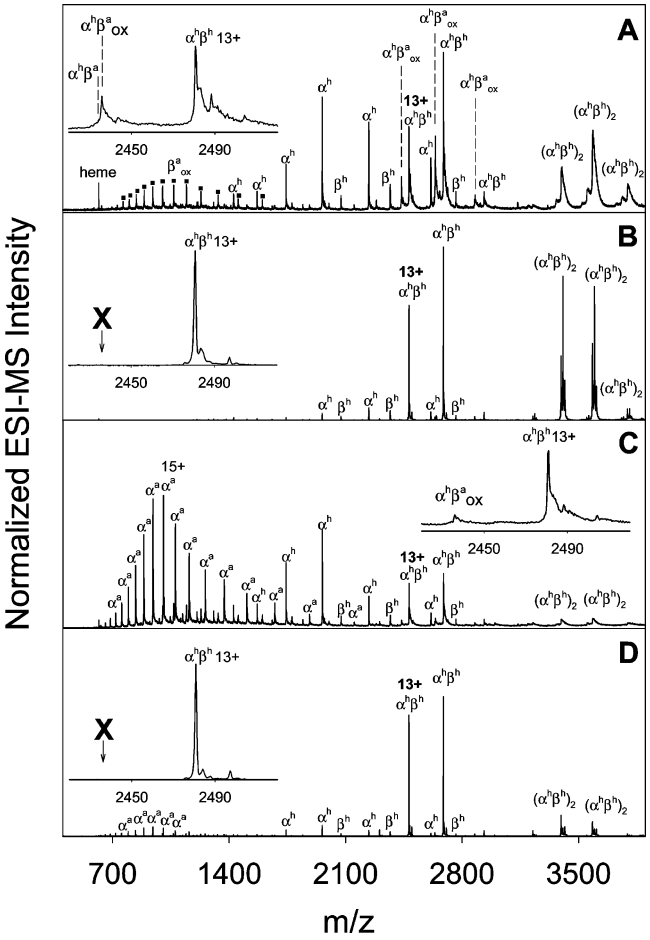

FIGURE 7: ESI mass spectra of commercially obtained ^{met}Hb (A) and freshly prepared ^{met}Hb (B) recorded at pH 5.8. Also shown are the corresponding data for pH 4.2 (C, commercial ^{met}Hb; D, freshly prepared ^{met}Hb). The insets focus on the *m*/*z* range corresponding to the 13+ heterodimer. The expected peak positions for $\alpha^h\beta^a{}_{ox}{}^{13+}$ and $\alpha^h\beta^a{}^{13+}$ are indicated as vertical dashed lines in the inset of panel (A). Arrows marked with "X" in (B) and (D) highlight the lack of $\alpha^h\beta^a$ and/or $\alpha^h\beta^a{}_{ox}$ in the spectra of freshly prepared ^{met}Hb.

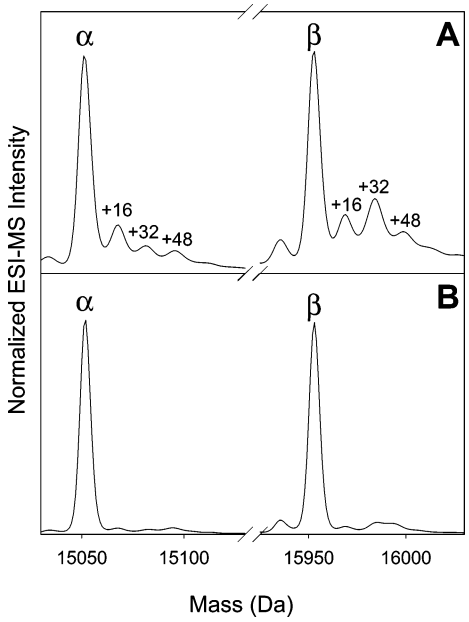

FIGURE 8: Deconvoluted mass distributions of α- and *β*-globin, obtained for acid-denatured ^{met}Hb at pH 2.1. (A) Commercial protein; (B) freshly prepared protein. The main peaks observed for each distribution correspond to the masses of unmodified α- and *β*-globin. Mass shifts of the observed covalent modifications are indicated. All four mass distributions have been normalized such that the base peak has roughly the same height in each case.

modification. MS/MS experiments verified the composition of this species as $\alpha^h\beta^a{}_{ox}$, ruling out other possible combinations that would result in the same mass such as $\alpha^a{}_{ox}\beta^h$ (*81*). Importantly, none of the freshly prepared Hb species investigated here exhibits significant levels of heme-deficient dimers when studied under native solvent conditions (Figure 1B−D). The same result is obtained when exposing the freshly prepared protein to semi-denaturing conditions. In the case of ^{oxy}Hb, this has already been demonstrated by the data in Figure 2. A direct comparison of ESI mass spectra for commercial and freshly prepared ^{met}Hb (i.e., using the same iron oxidation state in both cases) confirms the lack of $\alpha^h\beta^a$ and $\alpha^h\beta^a{}_{ox}$ for the freshly prepared protein, as exemplified for pH 5.8 (Figure 7A and B) and pH 4.2 (Figure 7C and D). Moreover, these data demonstrate that the commercial protein is less resistant to acid denaturation, as seen from the much higher intensity of monomeric globin chains in Figure 7C than in Figure 7D.

It is concluded that the asymmetric behavior (*46*) of the α- and *β*-subunits during acid-induced denaturation of commercial ^{met}Hb represents an artifact, likely caused by structural damage of the protein during isolation and/or storage. This apparent asymmetry seems to be largely caused by substantial levels of chemically altered *β*-globin (termed β_{ox}). The existence of $\alpha^h\beta^a{}_{ox}$ complexes implies that β_{ox} is still able to form noncovalent contacts with α^h, while exhibiting a greatly reduced heme affinity. However, the presence of a considerable fraction of free $\beta^a{}_{ox}$ under native conditions (Figure 1A) suggests that the interaction between α^h and $\beta^a{}_{ox}$ is relatively weak. Since the overall α/*β* stoichiometry in the sample is unity (*74*), the existence of free $\beta^a{}_{ox}$ necessarily leads to the presence of unbound α-globin. The latter maintains a compact heme-bound conformation, as seen by the low ESI charge states of α^h. In contrast, the lack of heme in $\beta^a{}_{ox}$ traps modified *β* chains in a non-native conformation (*12*) that is characterized by high ESI charge states (labeled with black squares in Figure 1A).

Identification of Oxidation Sites in Commercial ^{met}Hb. Deconvoluted mass distributions of acid-denatured ^{met}Hb provide an estimate of the overall level of covalent modifications. As expected from the data discussed above, the *β*-subunit of the commercial protein exhibits a dominant satellite peak that is shifted by +32 Da (Figure 8A). In addition, the *β*-globin mass distribution in Figure 8A exhibits less intense signals at +16 and +48 Da. These observations are attributed to the incorporation of one, two, or three oxygen atoms (*82*). Signals corresponding to up to three oxidation events also appear in the mass distribution of α-globin, albeit at lower levels. In contrast, the mass distributions of freshly prepared ^{met}Hb subunits recorded under identical conditions show only trace levels of oxidative modifications for both subunits (Figure 8B).

Tryptic peptide mapping was carried out in order to identify the locations of oxidation sites in commercial ^{met}Hb. Shown below are the sequences of bovine α- and *β*-globin, with trypsin cleavage sites indicated as spaces (*65*).

α-globin:

VLSAADK GNVK AAWGK VGGHAAEYGAEALER MFLSFPTTK TYFPHFDLSHGSAQVK GHGAK VAAALTK AVEHLDDLPGALSELSDLHAHK LRVDPVNFK LLSHSLLVTLASHLPSDFTPAVHASLDK FLANVSTVLTSK YR

β-globin:

MLTAEEK AAVTAFWGK VK VDEVGGEALGR LLVVYPWTQR FFESFGDLSTADAVMNNPK VK AHGK K VLDSFSNGMK HLDDLK GTFAALSELHCDK LHVDPENFK LLGN VLVVVLAR NFGK EFTPVLQADFQK VVAGVANALAHR YH

LC-MS revealed that all four methionine-containing tryptic peptides (one for α, three for β) were accompanied by derivatized variants carrying a +16 Da modification. None of the other peptides were found to carry +16 Da additions or multiples thereof. The oxidized species eluted at lower acetonitrile concentrations than the corresponding unmodified peptides (data not shown). This behavior reflects the fact that incorporation of oxygen increases the overall hydrophilicity of the modified peptides, resulting in less favorable interactions with the reverse-phase column (*82*). It was found that the intensity of the satellite peaks in Figure 8A depends somewhat on the experimental conditions, with higher ESI voltages leading to elevated oxidation levels. This phenomenon is attributed to redox reactions occurring during the ionization process, a common occurrence in ESI-MS (*83*). Importantly, however, the fact that oxidized and non-oxidized peptides can be separated on an LC column demonstrates the existence of oxidative modifications in bulk solution. Tandem mass spectrometry was used to confirm methionine as the site of oxidation in all four modified peptides. As an example, MS/MS data for the modified and unmodified peptide β6 are depicted in Figure 9. The masses of the C-terminal fragment ions up to y″4 are identical in both cases, whereas all fragments from y″5 onward show a mass shift of +16 Da. This confirms that methionine, the fifth residue from the C-terminus, carries the oxygen atom.

The observation of oxidized methionine residues is not particularly surprising, given the well-known susceptibility of this residue to oxidative damage by sulfoxide formation ($R\text{-}S\text{-}CH_3 \rightarrow R\text{-}SO\text{-}CH_3$) (*84*). It is interesting to note that no modifications were found for peptide β12, which contains cysteine as another potential oxidation site. However, this cysteine residue appears buried in the X-ray structure of the protein, whereas all three methionines in the β-subunit are partially solvent accessible. We note that low levels of non-methionine residues must be affected by oxidation as well, otherwise α-globin (carrying only one single Met) could not exhibit weak +32 and +48 Da signals (Figure 8A). Unfortunately, the identity of these low-level oxidation sites could not be uncovered in our MS/MS experiments. In summary, it appears that partial methionine oxidation is chiefly responsible for the different behavior of commercial and freshly prepared Hb during acid-induced denaturation. Oxidation of βMet54 (Figure 9A), located close to the $\alpha_1\beta_1$ interface, has previously been shown to destabilize the structure of $(\alpha^h\beta^h)_2$ (*85*). This provides an explanation for the significant level of monomeric globin chains for commercial ^{met}Hb under the conditions of Figure 1A. Our results suggest that methionine oxidation also interferes with the binding of β-globin to heme, evident from the presence of $\beta^a{}_{ox}$ and $\alpha^h\beta^a{}_{ox}$ in the spectra of the commercial protein (Figure 1A).

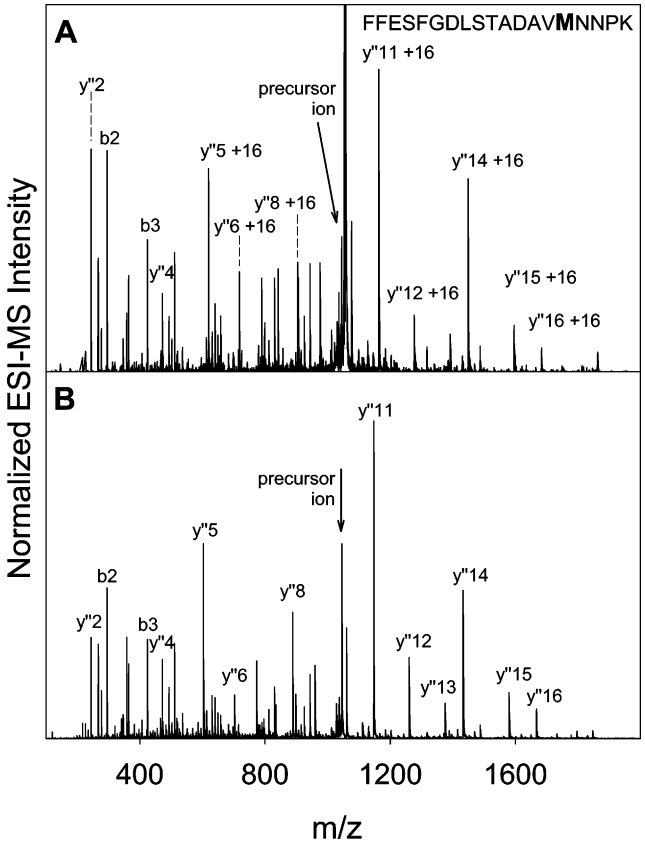

FIGURE 9: MS/MS spectra of the singly oxidized (A) and unmodified (B) tryptic peptide β6 obtained from commercial ^{met}Hb. The signals attributed to the doubly charged precursor ions (*m*/*z* 1053.47 and *m*/*z* 1045.48) are indicated, along with major singly charged fragment ions.

CONCLUSIONS

Earlier ESI-MS experiments sought to gain insights into the Hb assembly and disassembly mechanism by studying the protein at increasing acid concentrations (*46*). The results of that study suggested major differences in the behavior of α- and β-globin during pH denaturation. On the basis of those data, it was proposed that the assembly of $(\alpha^h\beta^h)_2$ follows a highly asymmetric mechanism. Unfortunately, the fact that those experiments were based on commercial ^{met}Hb casts doubts on the general validity of the conclusions reached. Our data reveal significant levels of oxidative damage in commercial ^{met}Hb. In contrast, oxidative modifications were almost absent in freshly prepared samples (Figure 8). Experiments on three freshly prepared Hb derivatives in the current study demonstrate that the responses of α and β to changes in pH are remarkably similar, as summarized in scheme 1. Thus, our work does not confirm the presence of a highly asymmetric Hb disassembly pathway upon acid denaturation.

It is not immediately clear whether experiments on the acid-induced denaturation of Hb *in vitro* have direct implications for the assembly of this protein complex at near-neutral pH and/or in a cellular environment, as suggested in ref *46*. The data presented here, therefore, do not rule out the possible occurrence of asymmetric (dis)assembly pathways under different conditions. In particular, the existence of a chaperone protein that specifically interacts with α-globin is consistent with an asymmetric mechanism *in vivo* (*8*, *23*−*28*). It appears that ESI-MS should be well suited to provide

detailed insights into the exact way in which this chaperone assists the assembly process of Hb in RBC precursors.

ACKNOWLEDGMENT

We thank Chris Buchner and family and Terry Boys for help with blood acquisition.

REFERENCES

1. Riggs, A. F. (1998) Self-association, cooperativity and supercooperativity of oxygen binding by hemoglobins, *J. Exp. Biol. 201*, 1073−1084.
2. Eaton, W. A., Henry, E. R., Hofrichter, J., and Mozzarelli, A. (1999) Is cooperative oxygen binding by hemoglobin really understood? *Nat. Struct. Biol. 6*, 351−358.
3. Perutz, M. F. (1970) Stereochemistry of cooperative effects in haemoglobin, *Nature 228*, 726−739.
4. Hardison, R. C. (1996) A brief history of hemoglobins: plant, animal, protist, and bacteria, *Proc. Nat. Acad. Sci. U.S.A. 93*, 5675−5679.
5. Antonini, E., and Brunori, M. (1971) *Hemoglobin and Myoglobin in Their Reactions With Ligands*, Vol. 21, North-Holland Publishing Company, Amsterdam.
6. Edelstein, S. J., Rehmar, M. J., Olson, J. S., and Gibson, Q. H. (1970) Functional aspects of the subunit association-dissociation equilibria of hemoglobin, *J. Biol. Chem. 245*, 4372−4381.
7. Schaeffer, J. R., McDonald, M. J., Turci, S. M., Dinda, D. M., and Bunn, H. F. (1984) Dimer-monomer dissociation of human hemoglobin A, *J. Biol. Chem. 259*, 14544−14547.
8. Santiveri, C. M., Perez-Canadillas, J. M., Viadivelu, M. K., Allen, M. D., Rutherford, T. J., Watkins, N. A., and Bycroft, M. (2004) NMR structure of the α-hemoglobin stabilizing protein, *J. Biol. Chem. 279*, 34963−34970.
9. White, S. L. (1975) The molecular dissociation of ferrihemoglobin derivatives, *J. Biol. Chem. 250*, 1263−1268.
10. Shaeffer, J. R., McDonald, M. J., and Bunn, H. F. (1981) Assembly of normal and abnormal human hemoglobins, *Trends Biochem. Sci. 6*, 158−161.
11. Rose, M. Y., and Olson, J. S. (1983) The kinetic mechanism of heme binding to human apohemoglobin, *J. Biol. Chem. 258*, 4298−4303.
12. Leutzinger, Y., and Beychok, S. (1981) Kinetics and mechanism of heme-induced refolding of human α-globin, *Proc. Natl. Acad. Sci. U.S.A. 78*, 780−784.
13. Adachi, K., Zhao, Y., and Surrey, S. (2003) Effects of heme addition on formation of stable human globin chains and hemoglobin subunit assembly in a cell-free system, *Arch. Biochem. Biophys. 413*, 99−106.
14. Hernan, R. A., and Sligar, S. G. (1995) Tetrameric hemoglobin expressed in *Escherichia coli*, *J. Biol. Chem. 270*, 26257−26264.
15. Joshi, A. A., and McDonald, M. J. (1994) Role of α and *β* carboxyl-terminal residues in the kinetics of human oxyhemoglobin dimer assembly, *J. Biol. Chem. 269*, 8549−8553.
16. McGovern, P., Reisberg, P., and Olson, J. S. (1976) Aggregation of deoxyhemoglobin subunits, *J. Biol. Chem. 251*, 7871−7879.
17. McDonald, M. J., Turci, S. M., Mrabet, N. T., Himelstein, B. P., and Bunn, H. F. (1987) The kinetics of assembly of normal and variant human oxyhemoglobins, *J. Biol. Chem. 262*, 5951−5956.
18. Kawamura, Y., Hasumi, H., and Nakamura, S. (1982) Kinetic studies on the reconstitution of deoxyhemoglobin from isolated α and *β* chains, *J. Biochem. 92*, 1227−1233.
19. Adachi, K., Yang, Y., Joshi, A. A., Vasudevan, G., Morris, A., and McDonald, M. J. (2001) Consequences of *β*16 and *β*112 replacements on the kinetics of hemoglobin assembly, *Biochem. Biophys. Res. Commun. 289*, 75−79.
20. Bunn, H. F., and McDonald, M. J. (1983) Electrostatic interactions in the assembly of haemoglobin, *Nature 306*, 498−500.
21. Mrabet, N. T., McDonald, M. J., Turci, S., Sarkar, R., Szabo, A., and Bunn, H. F. (1986) Electrostatic attraction governs the dimer assembly of human hemoglobin, *J. Biol. Chem. 261*, 5222−5228.
22. Yamaguchi, T., Yang, Y., McDonald, M. J., and Adachi, K. (2000) Surface and interface *β*-chain residues synergistically affect hemoglobin assembly, *Biochem. Biophys. Res. Commun. 270*, 683−687.
23. Luzzatto, L., and Notaro, R. (2002) Haemoglobin's chaperone, *Nature 417*, 703−704.
24. Kihm, A. J., Kong, Y., Hong, W., Russel, J. E., Rouda, S., Adachi, K., Simon, M. C., Blobel, G. A., and Weiss, M. J. (2002) An abundant erythroid protein that stabilizes free α-haemoglobin, *Nature 417*, 758−763.
25. Baudin-Creuza, V., Vasseur-Godbillon, C., Pato, C., Prehu, C., Wajcman, H., and Marden, M. C. (2004) Transfer of human α- to *β*-hemoglobin via its chaperone protein, *J. Biol. Chem. 279*, 36530−36533.
26. Hodge, D., Coghill, E., Keys, J., Maguire, T., Hartman, B., McDowall, A., Weiss, M., Grimmond, S., and Perkins, A. (2006) A global role for EKLF in definitive and primitive erythropoiesis, *Blood 15*, 3359−3370.
27. Feng, L., A., G. D., Zhou, S., Gu, L., Kong, Y., Li, J., Hu, M., Yan, N., Lee, C., Rich, A. M., Armstrong, R. S., Lay, P. A., Gow, A. J., Weiss, M. J., Mackay, J. P., and Shi, Y. (2004) Molecular mechanism of AHSP-mediated stabilization of α-hemoglobin, *Cell 119*, 629−640.
28. Feng, L., Zhou, S., Gu, L., Gell, D. A., Mackay, J. P., Weiss, M. J., Gow, A. J., and Shi, Y. (2005) Structure of oxidized α-haemoglobin bound to AHSP reveals a protective mechanism for haem, *Nature 435*, 697−701.
29. Boys, B. L., and Konermann, L. (2007) Folding and assembly of hemoglobin monitored by electrospray mass spectrometry using an on-line dialysis system, *J. Am. Soc. Mass Spectrom. 18*, 8−16.
30. Komar, A. A., Kommer, A., Krasheninnikov, I. A., and Spirin, A. S. (1997) Cotranslational folding of globin, *J. Biol. Chem. 272*, 10646−10651.
31. Komar, A. A., Kommer, A., Krasheninnikov, I. A., and Spirin, A. S. (1993) Cotranslational heme binding to nascent globin chains, *FEBS Lett. 326*, 261−263.
32. Vasudevan, G., and McDonald, M. J. (2002) Ordered heme binding ensures the assembly of fully functional hemoglobin: a hypothesis, *Curr. Protein Pept. Sci. 3*, 461−466.
33. Vasudevan, G., and McDonald, M. J. (1997) Spectral demonstration of semihemoglobin formation during CN-hemin incorporation into human apohemoglobin, *J. Biol. Chem. 272*, 517−524.
34. Vasudevan, G., and McDonald, M. J. (2006) Soret spectral and bioinformatic approaches provide evidence for a critical role of the α-subunit in assembly of tetrameric hemoglobin, *Protein J. 25*, 45−56.
35. Griffith, W. P., and Kaltashov, I. A. (2007) Protein conformational heterogeneity as a binding catalyst: ESI-MS study of hemoglobin H formation, *Biochemistry 46*, 2020−2026.
36. Kawamura-Konishi, Y., and Suzuki, H. (1985) Binding reaction of hemin to globin, *J. Biochem. 98*, 1181−1190.
37. Kawamura-Konishi, Y., Chiba, K., Kihara, H., and Suzuki, H. (1992) Kinetics of the reconstitution of hemoglobin from semihemoglobins α and *β* with heme, *Eur. Biophys. J. 21*, 85−92.
38. Kaltashov, I. A., and Eyles, S. J. (2002) Studies of biomolecular conformations and conformational dynamics by mass spectrometry, *Mass Spectrom. Rev. 21*, 37−71.
39. Heck, A. J. R., and Van den Heuvel, R. H. H. (2004) Investigation of intact protein complexes by mass spectrometry, *Mass Spectrom. Rev. 23*, 368−389.
40. Loo, J. A. (2005) in *The Encyclopedia of Mass Spectrometry* (Gross, M. L., and Caprioli, R. M., Eds.) pp 289−299, Elsevier, Amsterdam.
41. Ruotolo, B. T., and Robinson, C. V. (2006) Aspects of native proteins are retained in vacuum, *Curr. Opin. Chem. Biol. 10*, 402−408.
42. Smith, A. M., Jahn, T. R., Ashcroft, A. E., and Radford, S. E. (2006) Direct observation of oligomeric species formed in the early statges of amyloid formation using electrospray ionization mass spectrometry, *J. Mol. Biol. 364*, 9−19.
43. Potier, N., Donald, L. J., Chernushevich, I., Ayed, A., Ens, W., Arrowsmith, C. H., Standing, K. G., and Duckworth, H. W. (1998) Study of a noncovalent trp repressor: DNA operator complex by electrospray ionization time-of-flight mass spectrometry, *Protein Sci. 7*, 1388−1395.
44. Grandori, R., Matecko, I., and Muller, N. (2002) Uncoupled analysis of secondary and tertiary protein structure by circular dichroism and electrospray ionization mass spectrometry, *J. Mass Spectrom. 37*, 191−196.
45. Konermann, L. (2007) A minimalist model for exploring conformational effects on the electrospray charge state distribution of proteins, *J. Phys. Chem. B 111*, 6534−6543.
46. Griffith, W. P., and Kaltashov, I. A. (2003) Highly asymmetric interactions between globin chains during hemoglobin assembly

revealed by electrospray ionization mass spectrometry, *Biochemistry 42*, 10024−10033.
47. Griffith, W. P., and Kaltashov, I. A. (2006) Mass spectrometry in the study of hemoglobin: from covalent structure to higher order assembly, *Curr. Org. Chem. 10*, 535−553.
48. Light-Wahl, K. J., Schwartz, B. L., and Smith, R. D. (1994) Observation of the noncovalent quaternary association of proteins by electrospray ionization mass spectrometry, *J. Am. Chem. Soc. 116*, 5271−5278.
49. Schmidt, A., and Karas, M. (2001) The influence of electrostatic interactions on the detection of heme-globin complexes in ESI-MS, *J. Am. Soc. Mass Spectrom. 12*, 1092−1098.
50. Versluis, C., and Heck, A. J. R. (2001) Gas-phase dissociation of hemoglobin, *Int. J. Mass Spectrom. 210/211*, 637−649.
51. Mekecha, T. T., Amunugama, R., and McLuckey, S. A. (2006) Ion trap collision-induced dissociation of human hemoglobin α-chain cations, *J. Am. Soc. Mass Spectrom. 17*, 923−931.
52. Simmons, D. A., Wilson, D. J., Lajoie, G. A., Doherty-Kirby, A., and Konermann, L. (2004) Subunit disassembly and unfolding kinetics of hemoglobin studied by time-resolved electrospray mass spectrometry, *Biochemistry 43*, 14792−14801.
53. Hossain, B. M., and Konermann, L. (2006) Pulsed hydrogen/deuterium exchange MS/MS for studying the relationship between noncovalent protein complexes in solution and in the gas phase after electrospray ionization, *Anal. Chem. 78*, 1613−1619.
54. Shreffler, D. C., and Salisbury, G. W. (1959) Distribution of inheritance of hemoglobin variants in american cattle, *J. Dairy Sci. 42*, 1147−1156.
55. Paul, K. G., Theorell, H., and Akeson, A. (1953) The molar light absorption of pyridine ferroprotoporphyrin (pyridine haemochromogen), *Acta Chem. Scand. 7*, 1284−1287.
56. Crosby, W. H., and Houchin, D. N. (1957) Preparing standard solutions of cyanmethemoglobin, *Blood 12*, 1132−1136.
57. International Committee for Standardization in Haematology. (1978) Recommendations for reference method for haemoglobinometry in human blood (ICSH Standard EP 6/2:1977) and specifications for international haemiglobincyanide reference preparation (ICSH Standard EP 6/3:1977), *J. Clin. Pathol. 31*, 139−143.
58. Breepoel, P. M., Kreuzer, F., and Hazevoet, M. (1981) Interaction of Organic phosphates with bovine hemoglobin, *Pflugers Arch. 389*, 219−225.
59. Bunn, H. F. (1971) Differences in the interaction of 2,3-diphosphoglycerate with certain mammalian hemoglobins, *Science 172*, 1049−1050.
60. Moore, G. L., and et_al. (1992) Evaluation of methemoglobin formation during the storage of various hemoglobin solutions, *Artif. Organs 16*, 513−518.
61. Evelyn, K. A., and Malloy, H. T. Microdetermination of oxyhemoglobin, methemoglobin, and sulfhemoglobin in a single sample of blood, *J. Biol. Chem. 126*, 655−662.
62. Leahy, T., and Smith, R. (1960) Notes on methemoglobin determination, *Clin. Chem. 6*, 148−152.
63. Cruz-Laneira, A., Bal, B. J., Quintela, O., and Lopez-Rivadulla, M. (2002) Determination of methemoglobin and total hemoglobin in toxicological studies by derivative spectrophotometry, *J. Anal. Toxicol. 26*, 67−72.
64. Budaveri, S., Ed. (2006) *The Merck Index*, pp 4648, Merck & Co. Inc., Whitehouse station, NJ.
65. Mueser, T. C., Rogers, P. H., and Arnone, A. (2000) Interface sliding as illustrated by the multiple quaternary structures of liganded hemoglobin, *Biochemistry 39*, 15353−15364.
66. Ackers, G. K., and Halvorson, H. R. (1974) The linkage between oxygenation and subunit dissociation in human hemoglobin, *Proc. Natl. Acad. Sci. U.S.A. 71*, 4312−4316.
67. Lunelli, L., Paola, Z., and Baldini, G. (1994) Evidence of hemoglobin dissociation, *Biopolymers 34*, 747−757.
68. Peschke, M., Verkerk, U. H., and Kebarle, P. (2004) Features of the ESI mechanism that affect the observation of multiply charged noncovalent protein complexes and the determination of the association constant by the titration method, *J. Am. Soc. Mass Spectrom. 15*, 1424−1434.
69. Sun, J., Kitova, E. N., Wang, W., and Klassen, J. S. (2006) Method for distinguishing specific from nonspecific protein-ligand complexes in nanoelectrospray ionization mass spectrometry, *Anal. Chem. 78*, 3010−3018.
70. Green, B. N., and Vinogradov, S. N. (2004) An electrospray ionization mass spectrometric study of the subunit structure of the giant hemoglobin from the leech *Nephelopsis oscura*, *J. Am. Soc. Mass Spectrom. 15*, 22−27.
71. McKay, A. R., Ruotolo, B. T., Ilag, L. L., and Robinson, C. V. (2006) Mass measurements of increased accuracy resolve heterogeneous populations of intact ribosomes, *J. Am. Chem. Soc. 128*, 11433−11442.
72. Sen, U., Dasgupta, J., Choudhury, D., Datta, P., Chakrabarti, A., Chakrabarty, S. B., Chakrabarty, A., and Dattagupta, J. K. (2004) Crystal structure of HbA_2 and HbE and modeling of hemoglobin δ_4: interpretation of the thermal stability and the antisickling effect of HbA_2 and identification of the ferrocyanide binding site in Hb, *Biochemistry 43*, 12477−12488.
73. Dobo, A., and Kaltashov, I. A. (2001) Detection of multiple protein conformational ensembles in solution via deconvolution of charge-state distributions in ESI MS, *Anal. Chem. 73*, 4763−4773.
74. Kuprowski, M. C., Boys, B. L., and Konermann, L. (2007) Analysis of protein mixtures by electrospray mass spectrometry: effects of conformation and desolvation behavior on the signal intensities of hemoglobin subunits, *J. Am. Soc. Mass Spectrom. 18*, 1279−1285.
75. Sogbein, O. O., Simmons, D. A., and Konermann, L. (2000) The effects of pH on the kinetic reaction mechanism of myoglobin unfolding studied by time-resolved electrospray ionization mass spectrometry, *J. Am. Soc. Mass Spectrom. 11*, 312−319.
76. Adams, P. A. (1976) The kinetics and mechanism of the recombination reaction between apomyoglobin and haemin, *Biochem. J. 159*, 371−376.
77. Shikama, K. (2006) Nature of FeO_2 bonding in myoglobin and hemoglobin: a new molecular paradigm, *Prog. Biophys. Mol. Biol. 91*, 83−162.
78. Sage, J. T., Morikis, D., and Champion, P. M. (1991) Spectroscopic studies of myoglobin at low pH: heme structure and ligation, *Biochemistry 30*, 1227−1237.
79. Sage, J. T., Li, P., and Champion, P. M. (1991) Spectroscopic studies of myoglobin at low pH: heme ligation kinetics, *Biochemistry 30*, 1237−1247.
80. Konermann, L., Rosell, F. I., Mauk, A. G., and Douglas, D. J. (1997) Acid-induced denaturation of myoglobin studied by time-resolved electrospray ionization mass spectrometry, *Biochemistry 36*, 6448−6454.
81. Simmons, D. A., Dunn, S. D., and Konermann, L. (2003) Conformational dynamics of partially denatured myoglobin studied by time-resolved electrospray mass spectrometry with online hydrogen-deuterium exchange, *Biochemistry 42*, 5896−5905.
82. Takamono, K., and Chance, M. R. (2006) Radiolytic protein footprinting with mass spectrometry to probe the strucuture of macromolecular complexes, *Annu. Rev. Biophys. Biomol. Struct. 35*, 251−276.
83. Chen, M., and Cook, K. D. (2007) Oxidation artifacts in the electrospray mass spectrometry of Aβ peptide, *Anal. Chem. 79*, 2031−2036.
84. Creighton, T. E. (1993) *Proteins*, W. H. Freeman & Co., New York.
85. Amiconi, G., Ascoli, F., Barra, D., Bertollini, A., Matarese, R. M., Verzili, D., and Brunori, M. (1989) Selective oxidation of methionine β(55)D6 at the $\alpha 1\beta 1$ interface in hemoglobin completely destabilizes the T-state, *J. Biol. Chem. 264*, 17745−17749.

BI701076Q